Chapter 3
Koopman Analysis

Much of the interest surrounding DMD is due to its strong connection to nonlinear dynamical systems through Koopman spectral theory [196, 194, 235, 195]. The Koopman operator, introduced in 1931 by B. O. Koopman [162], is an infinite-dimensional linear operator that describes how measurements of a dynamical system evolve through the nonlinear dynamics. Because these measurements are functions, they form a Hilbert space, so the Koopman operator is infinite dimensional.

In 2009, Rowley et al. [235] demonstrated that under certain conditions, DMD provides a finite-dimensional approximation to eigenvalues and eigenvectors of the infinite-dimensional Koopman operator. In this chapter, we begin by providing an overview of spectral theory and eigenfunction expansions, first for finite-dimensional matrices and then for infinite-dimensional operators. Next, we introduce the Koopman operator and provide connections to DMD. Finally, we demonstrate the theory on two example dynamical systems.

3.1 ▪ Spectral theory and eigenfunction expansions

Before discussing the Koopman operator and its connection to DMD, it is important to review the basic ideas associated with spectral theory and eigenfunction expansion solutions of differential equations [98, 266]. We can consider this concept for both ordinary differential equations on vector spaces $\mathbb{R}^n$ and partial differential equations on function spaces $\mathscr{H}$. Recall that in the vector case, we are in general considering the nonlinear differential equation

$$\frac{d\mathbf{x}}{dt} = \mathbf{f}(\mathbf{x}, t; \mu). \tag{3.1}$$

The state $\mathbf{x} \in \mathbb{R}^n$ may be obtained by discretizing the state $\mathbf{u}$ of a partial differential equation (1.36) at a finite collection of discrete spatial locations. In this case, the dynamics approximate the partial differential equation (1.36) at these discrete locations.

3.1.1 ▪ Vector spaces

A traditional solution technique for such a problem is to use an eigenfunction expansion corresponding to a matrix $\mathbf{A}$ associated with either the linearization of (3.1) or

a natural coordinate system used to represent the dynamics (e.g., Fourier, Legendre polynomials). Thus, one can consider the eigenvalue problem

$$\mathbf{A}\mathbf{W} = \mathbf{W}\mathbf{\Lambda}, \tag{3.2}$$

where columns of $\mathbf{W}$ are the collection of eigenvectors ($\mathbf{w}_k$) and $\mathbf{\Lambda}$ is a diagonal matrix whose entries are the associated eigenvalues (λ_k). In addition to this eigenvalue problem, it is also necessary to consider the adjoint eigenvalue problem

$$\mathbf{A}^*\tilde{\mathbf{W}} = \tilde{\mathbf{W}}\tilde{\mathbf{\Lambda}}, \tag{3.3}$$

where $\mathbf{A}^*$ is the complex conjugate transpose of the matrix $\mathbf{A}$. More formally, the adjoint is defined such that

$$\left\langle \mathbf{A}\mathbf{x}_j, \mathbf{x}_k \right\rangle = \left\langle \mathbf{x}_j, \mathbf{A}^*\mathbf{x}_k \right\rangle, \tag{3.4}$$

where the inner product for vectors is defined by $\left\langle \mathbf{x}_j, \mathbf{x}_k \right\rangle = \mathbf{x}_k^*\mathbf{x}_j$. As before, the columns of $\tilde{\mathbf{W}}$ are the collection of eigenvectors ($\tilde{\mathbf{w}}_k$), and $\tilde{\mathbf{\Lambda}}$ is a diagonal matrix whose entries are the associated eigenvalues ($\tilde{\lambda}_k$). If the matrix $\mathbf{A}$ is self-adjoint, then the two eigenvalue problems are equivalent, since $\mathbf{A} = \mathbf{A}^*$. Note that the eigenvectors and adjoint eigenvectors satisfy the orthonormality conditions

$$\left\langle \mathbf{w}_j, \tilde{\mathbf{w}}_k \right\rangle = \delta_{jk} = \begin{cases} 1, & j = k, \\ 0, & j \neq k, \end{cases} \tag{3.5}$$

where δ_{jk} is the Dirac delta function. This can be easily seen by taking the inner product of $\mathbf{A}\mathbf{w}_j = \lambda_j \mathbf{w}_j$ with respect to $\tilde{\mathbf{w}}_k$, using the definition of the adjoint, and noting that $\lambda_j \neq \tilde{\lambda}_k$.

Spectral theory involves representing the solution to the differential equation (3.1) by the adjoint eigenvectors of the matrix $\mathbf{A}$. Specifically, one can posit a solution of the form

$$\mathbf{x}(t) = \sum_{k=1}^{n} a_k(t)\mathbf{w}_k, \tag{3.6}$$

where the coefficients $a_k = a_k(t)$ determine the time evolution of each eigenvector $\mathbf{w}_k$. This is an expression of the separation of variables. For linear systems, the time evolution of each eigenvector is directly linked to its eigenvalue λ_k, thus giving rise to the terminology *spectral theory*. Such spectral expansions can also be used to solve a linear system of equations for the unknown vector $\mathbf{x}$:

$$\mathbf{A}\mathbf{x} = \mathbf{b}. \tag{3.7}$$

Taking the inner product of both sides of (3.7) with respect to $\tilde{\mathbf{w}}_j$ gives

$$\begin{aligned}
&\left\langle \mathbf{A}\mathbf{x}, \tilde{\mathbf{w}}_j \right\rangle = \left\langle \mathbf{b}, \tilde{\mathbf{w}}_j \right\rangle, && \\
&\left\langle \mathbf{x}, \mathbf{A}^*\tilde{\mathbf{w}}_j \right\rangle = \left\langle \mathbf{b}, \tilde{\mathbf{w}}_j \right\rangle && \text{(definition of adjoint)}, \\
&\left\langle \mathbf{x}, \tilde{\lambda}_j\tilde{\mathbf{w}}_j \right\rangle = \left\langle \mathbf{b}, \tilde{\mathbf{w}}_j \right\rangle && \text{(use (3.3))}, \\
&\tilde{\lambda}_j^* \left\langle \mathbf{x}, \tilde{\mathbf{w}}_j \right\rangle = \left\langle \mathbf{b}, \tilde{\mathbf{w}}_j \right\rangle && \text{(pull out constant)}, \\
&\tilde{\lambda}_j^* \left\langle \sum_{k=1}^{n} a_k\mathbf{w}_k, \tilde{\mathbf{w}}_j \right\rangle = \left\langle \mathbf{b}, \tilde{\mathbf{w}}_j \right\rangle && \text{(expand with (3.6))}, \\
&\tilde{\lambda}_j^* a_j = \left\langle \mathbf{b}, \tilde{\mathbf{w}}_j \right\rangle && \text{(orthonormality)}.
\end{aligned}$$

The final expression allows for an explicit and unique computation of the weighting coefficients

$$a_j = \frac{\left\langle \mathbf{b}, \tilde{\mathbf{w}}_j \right\rangle}{\tilde{\lambda}_j^*}. \tag{3.8}$$

These n coefficients characterize the projection of the solution (3.6) onto the space $\mathbb{R}^n$ spanned by the eigenvectors. Note that when $\mathbf{A}$ is self-adjoint (i.e., $\mathbf{A} = \mathbf{A}^*$), then $\tilde{\lambda}_j^* = \lambda_j$.

When the expansion (3.6) is applied to the linear dynamical system

$$\frac{d\mathbf{x}}{dt} = \mathbf{A}\mathbf{x}, \tag{3.9}$$

the dynamics are diagonalized. Specifically, taking the inner product of this equation with respect to $\tilde{\mathbf{w}}_j$ gives

$$\begin{aligned}
&\left\langle \frac{d\mathbf{x}}{dt}, \tilde{\mathbf{w}}_j \right\rangle = \left\langle \mathbf{A}\mathbf{x}, \tilde{\mathbf{w}}_j \right\rangle, \\
&\left\langle \frac{d\mathbf{x}}{dt}, \tilde{\mathbf{w}}_j \right\rangle = \left\langle \mathbf{x}, \mathbf{A}^* \tilde{\mathbf{w}}_j \right\rangle && \text{(definition of adjoint)}, \\
&\left\langle \frac{d\mathbf{x}}{dt}, \tilde{\mathbf{w}}_j \right\rangle = \left\langle \mathbf{x}, \tilde{\lambda}_j \tilde{\mathbf{w}}_j \right\rangle && \text{(use (3.3))}, \\
&\left\langle \frac{d\mathbf{x}}{dt}, \tilde{\mathbf{w}}_j \right\rangle = \tilde{\lambda}_j^* \left\langle \mathbf{x}, \tilde{\mathbf{w}}_j \right\rangle && \text{(pull out constant)}, \\
&\left\langle \frac{d \sum_{k=1}^n a_k \mathbf{w}_k}{dt}, \tilde{\mathbf{w}}_j \right\rangle = \tilde{\lambda}_j^* \left\langle \sum_{k=1}^n a_k \mathbf{w}_k, \tilde{\mathbf{w}}_j \right\rangle && \text{(expand with (3.6))}, \\
&\left\langle \sum_{k=1}^n \frac{da_k}{dt} \mathbf{w}_k, \tilde{\mathbf{w}}_j \right\rangle = \tilde{\lambda}_j^* \left\langle \sum_{k=1}^n a_k \mathbf{w}_k, \tilde{\mathbf{w}}_j \right\rangle && \text{(derivative of coefficients)}, \\
&\frac{da_j}{dt} = \tilde{\lambda}_j^* a_j && \text{(orthonormality)}.
\end{aligned}$$

The last equation shows that the dynamics are diagonalized in the space of the adjoint eigenvectors.

Nonlinear dynamics (3.1) can also be represented by such eigenfunction expansions. In this case, taking the inner product of (3.1) with respect to $\tilde{\mathbf{w}}_j$ gives

$$\frac{da_j}{dt} = \left\langle \mathbf{f}(\mathbf{x}, t; \mu), \tilde{\mathbf{w}}_j \right\rangle, \tag{3.10}$$

where the right-hand side mixes eigenvectors through the inner product with the nonlinearity, i.e., the dynamics are no longer diagonalizable. Thus, the evolution of $a_j(t)$ depends in general on all $a_k(t)$, where $k = 1, 2, \ldots, n$. In numerical schemes, one can often choose a large enough set of basis modes ($n \gg 1$) to accurately compute the dynamics generated by the nonlinearity.

3.1.2 ▪ Function spaces

To set the foundations of Koopman theory, we must also consider function spaces and spectral theory for infinite-dimensional vector spaces. We need only consider the

linear partial differential equation for $q(x,t)$

$$\frac{dq}{dt} = \mathscr{L} q, \tag{3.11}$$

where $\mathscr{L}$ is a linear operator acting on an infinite-dimensional Hilbert space $\mathscr{H}$ of scalar functions on x. As with vector spaces, spectral theory revolves around two eigenvalue problems:

$$\mathscr{L} q_k = \lambda_k q_k, \tag{3.12a}$$

$$\mathscr{L}^* \tilde{q}_k = \tilde{\lambda}_k \tilde{q}_k, \tag{3.12b}$$

where $\mathscr{L}^*$ is the adjoint linear operator and q_k ($\tilde{q}_k$) and λ_k ($\tilde{\lambda}_k$) are the eigenfunctions (adjoint eigenfunctions) and eigenvalues (adjoint eigenvalues), respectively.

The eigenfunction solution can then be constructed as follows:

$$q(x,t) = \sum_{k=1}^{\infty} a_k(t) q_k(x), \tag{3.13}$$

where the $a_k(t)$ determine the weighting of each mode in the spectral representation of $q(x,t)$. The expansion can be used to solve the canonical problem equivalent to the vector space problem $\mathbf{Ax} = \mathbf{b}$,

$$\mathscr{L} q = f, \tag{3.14}$$

for a given right-hand side function $f(x)$. For example, this representation reduces to Laplace's equation when $\mathscr{L} = \nabla^2$ and $f = 0$ and Poisson's equation for nonzero f.

We define the inner product for functions as

$$\langle f, g \rangle = \int_{-\infty}^{\infty} f(x) g^*(x) dx. \tag{3.15}$$

Taking the inner product of the above with respect to $\tilde{q}_j$ yields

$$\begin{aligned}
&\left\langle \mathscr{L} q, \tilde{q}_j \right\rangle = \left\langle f, \tilde{q}_j \right\rangle, \\
&\left\langle q, \mathscr{L}^* \tilde{q}_j \right\rangle = \left\langle f, \tilde{q}_j \right\rangle && \text{(definition of adjoint)}, \\
&\left\langle q, \tilde{\lambda}_j \tilde{q}_j \right\rangle = \left\langle f, \tilde{q}_j \right\rangle && \text{(use (3.12))}, \\
&\tilde{\lambda}_j^* \left\langle q, \tilde{q}_j \right\rangle = \left\langle f, \tilde{q}_j \right\rangle && \text{(pull out constant)}, \\
&\tilde{\lambda}_j^* \left\langle \sum_{k=1}^{\infty} a_k(t) q_k(x), \tilde{q}_j \right\rangle = \left\langle f, \tilde{q}_j \right\rangle && \text{(expand with (3.13))}, \\
&\tilde{\lambda}_j^* a_j = \left\langle f, \tilde{q}_j \right\rangle && \text{(orthonormality)}.
\end{aligned}$$

The final expression again allows for an explicit and unique computation of the weighting coefficients

$$a_j = \frac{\left\langle f, \tilde{q}_j \right\rangle}{\tilde{\lambda}_j^*}. \tag{3.16}$$

These coefficients characterize the projection of the solution (3.13) onto the infinite-dimensional space spanned by the eigenfunctions.

Using a similar procedure, the linear differential equation (3.11) can be solved with a spectral representation. Taking the inner product of (3.11) with respect to $\tilde{q}_j$ yields

$$\begin{aligned}
&\left\langle \frac{dq}{dt}, \tilde{q}_j \right\rangle = \left\langle \mathscr{L}q, \tilde{q}_j \right\rangle, \\
&\left\langle \frac{dq}{dt}, \tilde{q}_j \right\rangle = \left\langle q, \mathscr{L}^* \tilde{q}_j \right\rangle && \text{(definition of adjoint)}, \\
&\left\langle \frac{dq}{dt}, \tilde{q}_j \right\rangle = \left\langle q, \tilde{\lambda}_j \tilde{q}_j \right\rangle && \text{(use (3.12))}, \\
&\left\langle \frac{dq}{dt}, \tilde{q}_j \right\rangle = \tilde{\lambda}_j^* \left\langle q, \tilde{q}_j \right\rangle && \text{(pull out constant)}, \\
&\left\langle \sum_{k=1}^{\infty} \frac{da_k}{dt} q_k, \tilde{q}_j \right\rangle = \tilde{\lambda}_j^* \left\langle \sum_{k=1}^{\infty} a_k q_k, \tilde{q}_j \right\rangle && \text{(expand with (3.13))}, \\
&\frac{da_j}{dt} = \tilde{\lambda}_j^* a_j && \text{(orthonormality)}.
\end{aligned}$$

The last equation shows that the linear dynamics are diagonalized in the space of the adjoint eigenfunctions, providing a simple spectral representation of the dynamics.

The vector and function space spectral expansions proceed in an almost identical manner. The important difference centers around the dimensionality. Specifically, the vector space is finite dimensional, of dimension n, while the function space is an infinite-dimensional Hilbert space. In practice, the infinite-dimensional space must be represented by a finite sum to be computationally tractable. For example, the Fourier series typically converges with relatively few terms. Importantly, the Koopman operator is *linear* and acts on infinite-dimensional function spaces. In contrast, the underlying dynamical system we are trying to characterize is typically nonlinear and constrained to finite vector spaces. The consequences of this are developed in what follows.

3.2 ▪ The Koopman operator

With spectral theory in hand, we can proceed to posit the fundamental concept behind the Koopman operator. The original work of Koopman in 1931 [162] considered Hamiltonian systems and formulated the Koopman operator in discrete time; however, we begin with continuous time and then derive the associated discrete-time formulation.

Definition: Koopman operator: *Consider a continuous-time dynamical system*

$$\frac{d\mathbf{x}}{dt} = \mathbf{f}(\mathbf{x}), \tag{3.17}$$

where $\mathbf{x} \in \mathscr{M}$ *is a state on a smooth* n*-dimensional manifold* $\mathscr{M}$*. The Koopman operator* $\mathscr{K}$ *is an infinite-dimensional linear operator that acts on all observable functions* $g : \mathscr{M} \to \mathbb{C}$ *so that*

$$\frac{d}{dt} g(\mathbf{x}) = \mathscr{K} g(\mathbf{x}) = \nabla g(\mathbf{x}) \cdot \mathbf{f}(\mathbf{x}) \tag{3.18}$$

Soon after the original paper, Koopman and von Neumann extended these results to dynamical systems with continuous spectra [163].

By definition, the Koopman operator is a *linear* operator that acts on the Hilbert $\mathcal{H}$ space of *all* scalar measurement functions g. As such, it is an infinite-dimensional operator. Thus, the transformation from the state-space representation of the dynamical system to the Koopman representation trades nonlinear, finite-dimensional dynamics for linear, infinite-dimensional dynamics. The advantage of such a trade-off is that we can solve linear differential equations using the spectral representation of the last section. Of course, an infinite-dimensional representation can be problematic, but in practice a sufficiently large, but finite, sum of modes is used to approximate the Koopman spectral solution. It should be noted that the definition (3.18) can be alternatively represented by a composition of the observables with the nonlinear evolution: $\mathcal{K}g = g \circ \mathbf{f}$.

The Koopman operator may also be defined for discrete-time dynamical systems, which are more general than continuous-time systems. In fact, the dynamical system in (3.17) will induce a discrete-time dynamical system given by the flow map $\mathbf{F}_t : \mathcal{M} \to \mathcal{M}$, which maps the state $\mathbf{x}(t_0)$ to a future time $\mathbf{x}(t_0 + t)$:

$$\mathbf{F}_t(\mathbf{x}(t_0)) = \mathbf{x}(t_0 + t) = \mathbf{x}(t_0) + \int_{t_0}^{t_0+t} \mathbf{f}(\mathbf{x}(\tau))\, \mathbf{d}\tau. \tag{3.19}$$

This induces the discrete-time dynamical system

$$\mathbf{x}_{k+1} = \mathbf{F}_t(\mathbf{x}_k), \tag{3.20}$$

where $\mathbf{x}_k = \mathbf{x}(k\,t)$. The analogous discrete-time Koopman operator is given by $\mathcal{K}_t$ such that $\mathcal{K}_t g = g \circ \mathbf{F}_t$. Thus, the Koopman operator sets up a discrete-time dynamical system on the observable function g:

$$\mathcal{K}_t g(\mathbf{x}_k) = g(\mathbf{F}_t(\mathbf{x}_k)) = g(\mathbf{x}_{k+1}). \tag{3.21}$$

The spectral decomposition of the Koopman operator will be instrumental in representing solutions to a dynamical system of interest. Thus, we consider the eigenvalue problem

$$\mathcal{K}\varphi_k = \lambda_k \varphi_k. \tag{3.22}$$

The functions $\varphi_k(\mathbf{x})$ are Koopman eigenfunctions, which define a set of intrinsic measurement coordinates, on which it is possible to advance these measurements with a *linear* dynamical system. As was shown previously, one can represent the evolution of the dynamics, in this case on the observables, using an eigenfunction expansion solution of the Koopman operator.

A vector of observables $\mathbf{g}$ may be written in terms of Koopman eigenfunctions φ as

$$\mathbf{g}(\mathbf{x}) = \begin{bmatrix} g_1(\mathbf{x}) \\ g_2(\mathbf{x}) \\ \vdots \\ g_p(\mathbf{x}) \end{bmatrix} = \sum_{k=1}^{\infty} \varphi_k(\mathbf{x})\mathbf{v}_k, \tag{3.23}$$

where $\mathbf{v}_k$ is the kth Koopman mode associated with the kth Koopman eigenfunction φ_k. In the original theory [162], Koopman considered Hamiltonian flows that are

measure preserving, so that the Koopman operator is unitary. In this case, the eigenfunctions are all orthonormal, and (3.23) may be written explicitly as

$$\mathbf{g}(\mathbf{x}) = \sum_{k=1}^{\infty} \varphi_k(\mathbf{x}) \begin{bmatrix} \langle \varphi_k, g_1 \rangle \\ \langle \varphi_k, g_2 \rangle \\ \vdots \\ \langle \varphi_k, g_p \rangle \end{bmatrix} = \sum_{k=1}^{\infty} \varphi_k(\mathbf{x}) \mathbf{v}_k. \tag{3.24}$$

DMD is used to approximate the Koopman eigenvalues λ_k and modes $\mathbf{v}_k$, as we will show in the next section.

The critical insight to be gained in this transformation is that the finite-dimensional, nonlinear dynamical system defined by $\mathbf{f}$ in (3.17) and the infinite-dimensional, linear dynamics defined by $\mathcal{K}$ in (3.18) are two equivalent representations of the same fundamental behavior. Critical to the success of the Koopman theory is the ability to link the observables $\mathbf{g}$ and the associated Koopman mode expansion to the original evolution defined by $\mathbf{f}$. Under suitable conditions, this can be accomplished, as will be shown in what follows. Note that this representation is highly advantageous. Specifically, one can either evolve the system in the original state space (3.17), requiring computational effort since it is nonlinear, or one can instead evolve using (3.18) and (3.23) so that

$$\mathcal{K}\mathbf{g}(\mathbf{x}) = \mathcal{K} \sum_{k=1}^{\infty} \varphi_k(\mathbf{x}) \mathbf{v}_k = \sum_{k=1}^{\infty} \mathcal{K} \varphi_k(\mathbf{x}) \mathbf{v}_k = \sum_{k=1}^{\infty} \lambda_k \varphi_k(\mathbf{x}) \mathbf{v}_k. \tag{3.25}$$

Thus, future solutions can be computed by simple multiplication with the Koopman eigenvalue. Importantly, the Koopman operator captures everything about the nonlinear dynamical system (3.17), and its eigenfunctions define a nonlinear change of coordinates in which the system becomes linear.

Indeed, if we restrict our observable functions g to an invariant subspace spanned by eigenfunctions of the Koopman operator, then this induces a linear operator $\mathbf{K}$ that is finite dimensional and advances these eigenobservable functions on this subspace [45]. This is illustrated in Figure 3.1. Finding eigenfunctions of the Koopman operator and obtaining finite-dimensional models is both challenging and rewarding. Even knowing which terms in the dynamical system are active may be a challenge, although new techniques from machine learning identify relevant terms in the dynamics from data [252, 295, 47].

It was shown recently that level sets of the Koopman eigenfunctions form invariant partitions of the state-space for a given dynamical system [51]. This result implies that Koopman eigenfunctions may be used to represent and analyze the ergodic partition [197, 50]. Another important result shows that Koopman analysis is able to generalize and extend the Hartman–Grobman theorem to the entire basin of attraction of a stable or unstable equilibrium point or periodic orbit [170]. More detailed and in-depth discussion of these topics are covered in the excellent reviews by Mezić et al. [52, 195].

It is worth noting that the adjoint of the Koopman operator is the Perron–Frobenius operator, which is frequently used to analyze the flow of probability densities through a dynamical system [79, 100, 102, 101]. Perron–Frobenius computations are often related to the calculation of almost-invariant sets [102, 103, 274, 303] using set-oriented methods [79, 80] to identify eigenvectors of the Perron–Frobenius operator. Almost-invariant sets are useful to understand sensitivity and coherence in fluid systems and also have relevance to uncertainty quantification.

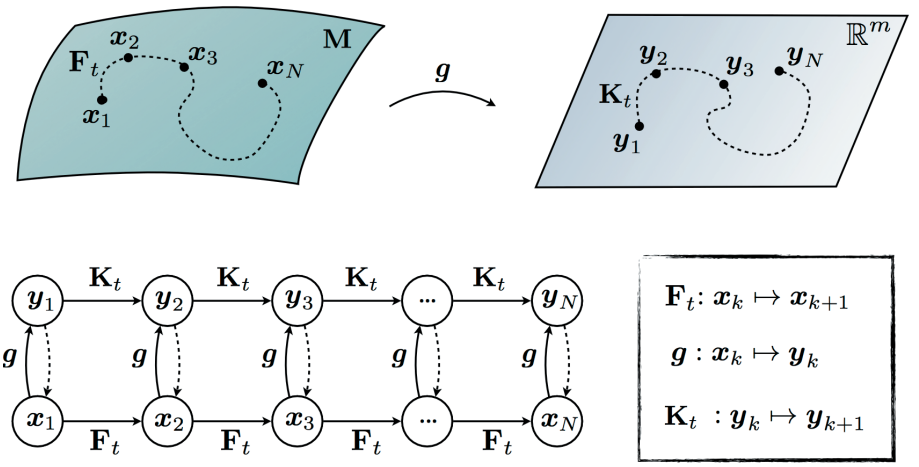

Figure 3.1. *Schematic illustrating the Koopman operator restricted to a finite-dimensional invariant subspace spanned by eigenobservable functions. The restriction of $\mathscr{K}$ to this subspace results in* $\mathbf{K}$*, which induces a finite-dimensional linear system on the invariant subspace. Reprinted with permission from the Public Library of Science* [45].

3.3 ▪ Connections with DMD

The DMD algorithm determines the Koopman eigenvalues and modes directly from data under suitable conditions. Specifically, the choice of observables will play a critical role in the success of the Koopman method [301]. Figure 3.2 shows the standard DMD approach and contrasts it with the Koopman mode decomposition. Before demonstrating the connection, we recall the definition of the DMD method [290].

Definition: DMD (Tu et al. 2014 [290]): *Suppose we have a dynamical system* (3.17) *and two sets of data,*

$$\mathbf{X} = \begin{bmatrix} | & | & & | \\ \mathbf{x}_1 & \mathbf{x}_2 & \cdots & \mathbf{x}_{m-1} \\ | & | & & | \end{bmatrix}, \tag{3.26a}$$

$$\mathbf{X}' = \begin{bmatrix} | & | & & | \\ \mathbf{x}'_1 & \mathbf{x}'_2 & \cdots & \mathbf{x}'_{m-1} \\ | & | & & | \end{bmatrix}, \tag{3.26b}$$

with $\mathbf{x}_k$ an initial condition to (3.17) *and $\mathbf{x}'_k$ its corresponding output after some prescribed evolution time Δt, with $m-1$ initial conditions considered. The DMD modes are eigenvectors of*

$$\mathbf{A}_{\mathbf{X}} = \mathbf{X}'\mathbf{X}^{\dagger}, \tag{3.27}$$

where † denotes the Moore–Penrose pseudoinverse.

With this definition, we can now more formally consider the set of p observables

$$g_j : \mathscr{M} \to \mathbb{C}, \qquad j = 1, 2, \ldots, p\,. \tag{3.28}$$

We let $\mathbf{g} = [g_1 \; g_2 \; \cdots \; g_p]^T$ denote the column vector of observables. We now construct data matrices $\mathbf{Y}$ and $\mathbf{Y}'$ by considering a set of initial conditions $\{\mathbf{x}_1 \; \mathbf{x}_2 \; \cdots \; \mathbf{x}_{m-1}\}$

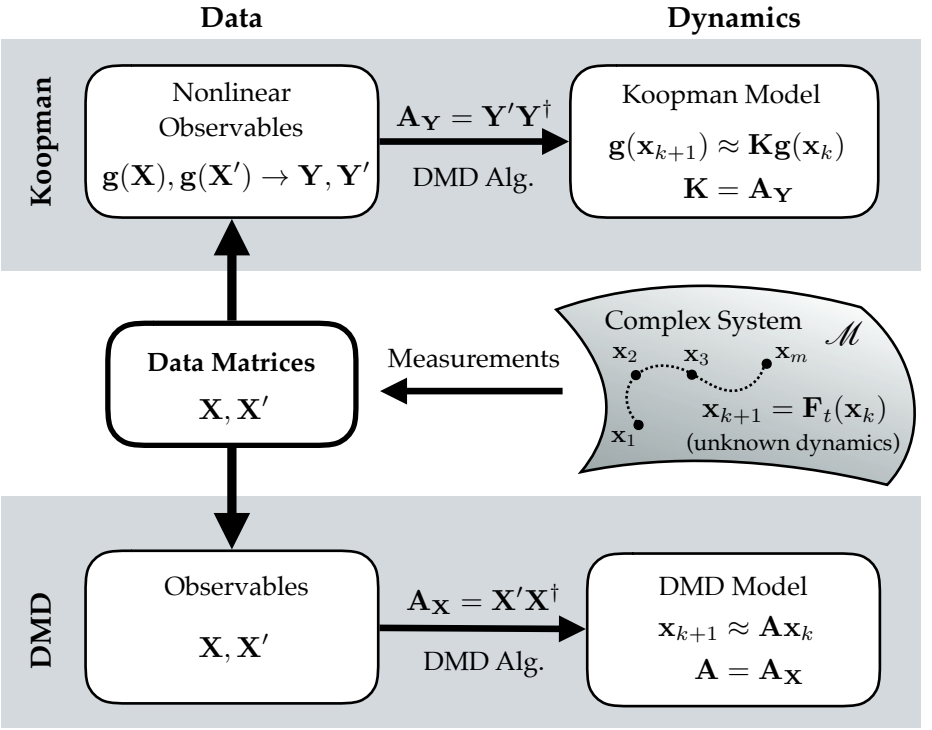

Figure 3.2. *Schematic of how to use data to generate dynamical systems models of an unknown complex system in the DMD/Koopman framework. In standard DMD, we take measurements of the states of the system and construct a model that maps* $\mathbf{X}$ *to* $\mathbf{X}'$*. Koopman spectral analysis enriches the measurements with nonlinear observations* $\mathbf{y} = \mathbf{g}(\mathbf{x})$ *to provide a better mapping from* $\mathbf{Y}$ *to* $\mathbf{Y}'$ *that approximates the infinite-dimensional Koopman mapping. The prediction of the observables in the future from the Koopman model may be used to recover the future state* $\mathbf{x}_{m+1}$*, provided that the observation function* $\mathbf{g}$ *is injective. Both the DMD and Koopman approaches are equation-free, in that they do not rely on knowing* $\mathbf{F}_t$*.*

to (3.17). The columns of the matrix $\mathbf{Y}$ are given by $\mathbf{y}_k = \mathbf{g}(\mathbf{x}_k)$. The columns of $\mathbf{Y}'$ are given by evolving (3.17) forward in time a prescribed time Δt and viewing the output vector through the observables, denoted by $\mathbf{y}'_k = \mathbf{g}(\mathbf{x}'_k)$. The resulting DMD algorithm on the data of observables produces $\mathbf{A_Y} = \mathbf{Y}'\mathbf{Y}^\dagger$, which gives the requisite Koopman approximation. The procedure, and its comparison to the standard DMD method, are shown in Figure 3.2. Note that $\mathbf{Y}$ and $\mathbf{Y}'$ compute DMD on the space of observables instead of on the state-space. We can now introduce the following theorem [235, 290, 237, 301].

Theorem: Koopman mode decomposition and DMD: *Let* φ_k *be an eigenfunction of* $\mathcal{K}$ *with eigenvalue* λ_k*, and suppose* $\varphi_k \in span\{g_j\}$*, so that*

$$\varphi_k(\mathbf{x}) = w_1 g_1(\mathbf{x}) + w_2 g_2(\mathbf{x}) + \cdots + w_p g_p(\mathbf{x}) = \mathbf{w} \cdot \mathbf{g} \tag{3.29}$$

for some $\mathbf{w} = [w_1 \ w_2 \ \cdots \ w_p]^T \in \mathbb{C}^p$*. If* $\mathbf{w} \in R(\mathbf{Y})$*, where* R *is the range, then* $\mathbf{w}$ *is a left eigenvector of* $\mathbf{A_Y}$ *with eigenvalue* λ_k *so that* $\tilde{\mathbf{w}}^* \mathbf{A_Y} = \lambda_k \tilde{\mathbf{w}}^*$*.*

This thus shows that the Koopman eigenvalues are the DMD eigenvalues provided (i) the set of observables is sufficiently large so that $\varphi_k(\mathbf{x}) \in \text{span}\{g_j\}$ and (ii) the data is sufficiently *rich* so that $\mathbf{w} \in R(\bar{\mathbf{X}})$. This directly shows that the choice of observables is critical in allowing one to connect DMD theory to Koopman spectral analysis. If this can be done, then one can simply take data snapshots of a finite-dimensional nonlinear dynamical system in time and reparameterize it as linear, infinite-dimensional system that is amenable to a simple eigenfunction (spectral) decomposition. This representation diagonalizes the dynamics and shows that the time evolution of each eigenfunction corresponds to multiplication by its corresponding eigenvalue.

3.3.1 ▪ Finite approximation of the Koopman operator

The above definitions provide an abstract framing of the Koopman theory. Note that to compute many of the meaningful quantities in Figure 3.2 would require knowledge of the right-hand side $\mathbf{f}(\cdot)$ in (3.17). But the fact that we do not know the prescribed evolution is precisely why we are using the DMD framework.

In practice, we must consider three important practical constraints: (i) we have data $\mathbf{X}$ and $\mathbf{X}'$, but we do not know $\mathbf{f}(\cdot)$; (ii) we will have to make a finite-dimensional approximation to the infinite-dimensional Koopman operator $\mathcal{K}$; and (iii) we will have to judiciously select the observables $g(\mathbf{x})$ to have confidence that the Koopman operator will approximate the nonlinear dynamics of $\mathbf{f}(\cdot)$. Points (i) and (ii) go naturally together. Specifically, the number of measurements in each column of $\mathbf{X}$ and $\mathbf{X}'$ is n, while the number of total columns (time measurements) is m. Thus finite-dimensionality is imposed simply from the data collection limitations. The dimension can be increased with a large set of observables, or it can be decreased via a low-rank truncation during the DMD process. The observables are more difficult to deal with in a principled way. Indeed, a good choice of observables can make the method extremely effective, but it would also require expert knowledge of the system at hand. This will be discussed further in the examples.

The following gives a practical demonstration of how to use the data and the observables to produce a Koopman operator and a future-state prediction of the nonlinear evolution (3.17). It should be compared to the DMD algorithm on the space of state-space variables introduced in the introduction. Essentially, the algorithm now needs to be applied in the space of observables.

1. First, from the data matrices $\mathbf{X}$ and $\mathbf{X}'$, create the data matrices of observables $\mathbf{Y}$ and $\mathbf{Y}'$:

$$\mathbf{Y} = \begin{bmatrix} | & | & & | \\ \mathbf{g}(\mathbf{x}_1) & \mathbf{g}(\mathbf{x}_2) & \cdots & \mathbf{g}(\mathbf{x}_{m-1}) \\ | & | & & | \end{bmatrix}, \tag{3.30a}$$

$$\mathbf{Y}' = \begin{bmatrix} | & | & & | \\ \mathbf{g}(\mathbf{x}'_1) & \mathbf{g}(\mathbf{x}'_2) & \cdots & \mathbf{g}(\mathbf{x}'_{m-1}) \\ | & | & & | \end{bmatrix}, \tag{3.30b}$$

   where each column is given by $\mathbf{y}_k = \mathbf{g}(\mathbf{x}_k)$ or $\mathbf{y}'_k = \mathbf{g}(\mathbf{x}'_k)$.

2. Next, perform the DMD algorithm to compute

$$\mathbf{A}_{\mathbf{Y}} = \mathbf{Y}'\mathbf{Y}^{\dagger} \tag{3.31}$$

along with the low-rank counterpart $\tilde{\mathbf{A}}_{\mathbf{Y}}$. The eigenvalues and eigenvectors of $\mathbf{A}_{\mathbf{Y}}$ may approximate Koopman eigenvalues and modes, depending on the set of observables chosen.

3. DMD can be used to compute the augmented modes $\mathbf{\Phi}_{\mathbf{Y}}$, which may approximate the Koopman modes, by (see step 4 in the DMD algorithm)

$$\mathbf{\Phi}_{\mathbf{Y}} = \mathbf{Y}'\mathbf{V}\mathbf{\Sigma}^{-1}\mathbf{W}, \tag{3.32}$$

where $\mathbf{W}$ comes from the eigenvalue problem $\tilde{\mathbf{A}}_{\mathbf{Y}}\mathbf{W} = \mathbf{W}\mathbf{\Lambda}$ and $\mathbf{Y} = \mathbf{U}\mathbf{\Sigma}\mathbf{V}^*$.

4. The future state in the space of observables is then given by the linear evolution

$$\mathbf{y}(t) = \mathbf{\Phi}_{\mathbf{Y}}\,\mathrm{diag}(\exp(\boldsymbol{\omega} t))\mathbf{b}, \tag{3.33}$$

where $\mathbf{b} = \mathbf{\Phi}_{\mathbf{Y}}^{\dagger}\mathbf{y}_1$ is determined by projecting back to the initial data observable, and $\boldsymbol{\omega}$ are the set of eigenvalues λ_k generated from the matrix $\mathbf{\Lambda}$, where $\omega_k = \ln(\lambda_k)/\Delta t$.

5. Transform from observables back to state-space:

$$\mathbf{y}_k = \mathbf{g}(\mathbf{x}_k) \quad \rightarrow \quad \mathbf{x}_k = \mathbf{g}^{-1}(\mathbf{y}_k). \tag{3.34}$$

This last step can be trivial if one of the observables selected to comprise $\mathbf{g}(\mathbf{x}_k)$ is the state variable $\mathbf{x}_k$ itself. If only nonlinear observables of $\mathbf{x}_k$ are chosen, then the inversion process can be difficult.

This process shows that the DMD algorithm is closely related to the Koopman operator. Indeed, it is the foundational piece for practical evaluation of the finite-dimensional Koopman operator. We stress once again that selection of appropriate observables is critical for the algorithm to generate good approximation to the future state.

3.4 ▪ Example dynamical systems

The success of the Koopman theory relies primarily on expert-in-the-loop choices of the observables $\mathbf{g}(\mathbf{x})$. In what follows, we introduce a couple of examples where an attempt is made to show how a future state is approximated using standard DMD on state variables versus the Koopman decomposition on the observables. The starting point is a one-dimensional example that can be worked out in complete detail. We finish with a partial differential equations example using the completely data-driven approach illustrated in Figure 3.2.

3.4.1 ▪ One-degree-of-freedom system

The simplest example of the Koopman framework can be demonstrated with the stable, one-degree-of-freedom system

$$\frac{dx}{dt} = -\mu x \tag{3.35}$$

whose solution is $x(t) = x(0)\exp(-\mu t)$, where $x(0)$ is the initial condition. Thus, the future state of the system can be found in the state-space representation by simple multiplication of the initial condition by $\exp(-\mu t)$.

For this example, we define the observable

$$g(x) = x \tag{3.36}$$

and note that

$$\mathcal{K}\, g(x) = g(x\exp(-\mu t)) \;\rightarrow\; \mathcal{K}\, x = x\exp(-\mu t). \tag{3.37}$$

This shows that the Koopman eigenfunction and eigenvalue are given by

$$\varphi_1 = x, \tag{3.38a}$$
$$\lambda_1 = -\mu. \tag{3.38b}$$

This result illustrates the fact that the eigenvalues for linearly stable systems are contained within the spectrum of the Koopman operator [235].

However, the set of eigenvalues of the Koopman operator is larger than that of the linear ones, and it depends on the space of functions in which the evolution is taking place [104]. To demonstrate this, consider instead the observable

$$g(x) = x^n, \tag{3.39}$$

where $n \in \mathbb{Z}^+$. In this case,

$$\mathcal{K}\, g(x) = g(x\exp(-\mu t)) \;\rightarrow\; \mathcal{K}\, x^n = x^n \exp(-n\mu t) \tag{3.40}$$

or, in observable notation,

$$\mathcal{K}\, g(x) = \exp(-n\mu t) g(x). \tag{3.41}$$

This gives the Koopman eigenfunction and eigenvalue

$$\varphi_n = x^n, \tag{3.42a}$$
$$\lambda_n = -n\mu. \tag{3.42b}$$

Any observable can then be found by the expansion

$$g(x) = \sum_{k=1}^{\infty} \mathbf{v}_k x^k \tag{3.43}$$

with solution at time t in the future given by

$$\mathcal{K}\, g(x) = \sum_{k=1}^{\infty} \mathbf{v}_k \exp(-k\mu t) x^k. \tag{3.44}$$

This simplest of examples illustrates how the Koopman space of eigenfunctions is actually infinite dimensional, with a spanning set that is much larger than one might initially think. Moreover, this space is directly tied to the observables used to investigate the system.

3.4.2 ▪ Nonlinear dynamical system

Now consider the following nonlinear ordinary differential equation in two variables:

$$\dot{x}_1 = \mu x_1, \tag{3.45a}$$
$$\dot{x}_2 = \lambda(x_2 - x_1^2). \tag{3.45b}$$

If $\lambda \ll |\mu| < 0$, then the dynamics of x_2 converge rapidly to x_1^2, so that $x_2 = x_1^2$ is a slow manifold. This example has been used to demonstrate the ability of the Koopman operator to capture nonlinear dynamics in terms of a linear operator on nonlinear measurements of the state $\mathbf{x}$ [290, 45]. In particular, if we restrict the Koopman operator to an observable subspace spanned by the measurements x_1, x_2, and x_1^2, then we obtain a *linear* dynamical system on these three states that advances the original state $\mathbf{x}$:

$$\begin{bmatrix} y_1 \\ y_2 \\ y_3 \end{bmatrix} = \begin{bmatrix} x_1 \\ x_2 \\ x_1^2 \end{bmatrix} \quad \Longrightarrow \quad \frac{d}{dt}\begin{bmatrix} y_1 \\ y_2 \\ y_3 \end{bmatrix} = \underbrace{\begin{bmatrix} \mu & 0 & 0 \\ 0 & \lambda & -\lambda \\ 0 & 0 & 2\mu \end{bmatrix}}_{\mathbf{K}} \begin{bmatrix} y_1 \\ y_2 \\ y_3 \end{bmatrix}. \tag{3.46}$$

This procedure of including higher-order powers of the state, as in $y_3 = x_1^2$, is closely related to the Carleman linearization [61, 267, 164], which has extensions to nonlinear control [37, 16, 270].

By looking at left eigenvectors $\tilde{\varphi}_\alpha$ of the Koopman operator $\mathbf{K}$ corresponding to eigenvalues α,

$$\tilde{\varphi}_\alpha^* \mathbf{K} = \alpha \tilde{\varphi}_\alpha^*, \tag{3.47}$$

it is possible to obtain eigenfunction measurements $\varphi_\alpha(\mathbf{x}) = \tilde{\varphi}_\alpha^* \mathbf{y}(\mathbf{x})$, which are intrinsic coordinates. For this example, $\varphi_\mu = x_1$ and $\varphi_\lambda = x_2 - b x_1^2$, where $b = \lambda/(\lambda - 2\mu)$ parameterizes how aggressively the slow manifold attracts trajectories.

***ALGORITHM* 3.1. Generate data for a nonlinear dynamical system.**

```
mu = -.05;
lambda = -1;
A = [mu 0 0; 0 lambda -lambda; 0 0 2*mu];  % Koopman linear
    dynamics
[T,D] = eig(A);
slope_stab_man = T(3,3)/T(2,3);  % slope of stable subspace (
    green)

%% Integrate Koopman trajectories
y0A = [1.5; -1; 2.25];
y0B = [1; -1; 1];
y0C = [2; -1; 4];
tspan = 0:.01:1000;
[t,yA] = ode45(@(t,y)A*y,tspan,y0A);
[t,yB] = ode45(@(t,y)A*y,tspan,y0B);
[t,yC] = ode45(@(t,y)A*y,tspan,y0C);
```

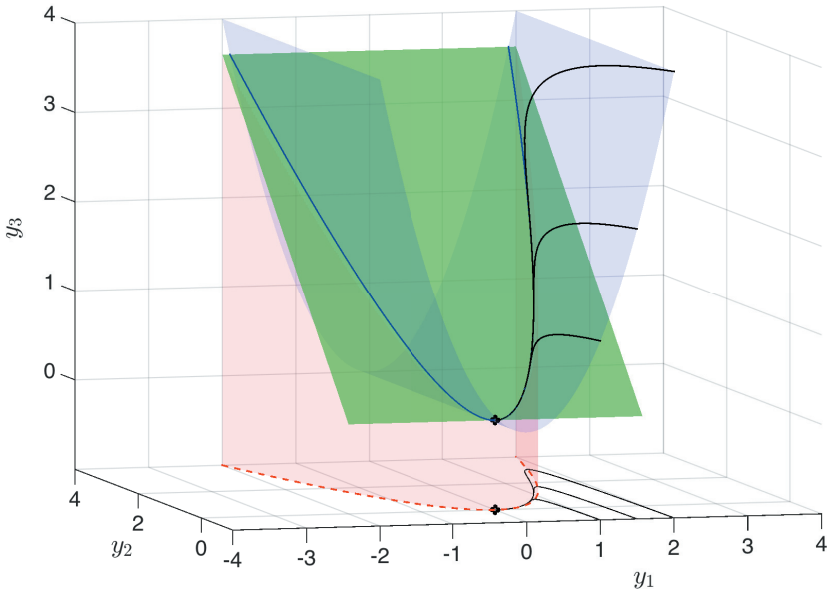

Figure 3.3. *Visualization of three-dimensional linear Koopman system from* (3.46) *(black curves). Projected onto the x_1-x_2 plane, these black curves represent solutions to the nonlinear dynamical system in* (3.45a). *Trajectories attract rapidly onto the slow manifold (red). The three-dimensional linear system has a slow subspace (green), and trajectories are also constrained to start on the level set $y_3 = y_1^2$ (blue). In this example, $\mu = -0.05$ and $\lambda = 1$. Reprinted with permission from the Public Library of Science* [45].

***ALGORITHM* 3.2. Plot Koopman linearization of nonlinear dynamical system.**

```
% Attracting manifold $y_2=y_1^2$ (red manifold)
[X,Z] = meshgrid(-2:.01:2,-1:.01:4);
Y = X.^2;
surf(X,Y,Z,'EdgeColor','None','FaceColor','r','FaceAlpha',.1)
hold on, grid on, view(-15,8), lighting gouraud

% Invariant set $y_3=y_1^2$ (blue manifold)
[X1,Y1] = meshgrid(-2:.01:2,-1:.01:4);
Z1 = X1.^2;
surf(X1,Y1,Z1,'EdgeColor','None','FaceColor','b','FaceAlpha',.1)

% Stable invariant subspace of Koopman linear system (green
    plane)
[X2,Y2]=meshgrid(-2:0.01:2,0:.01:4);
Z2 = slope_stab_man*Y2;  % for mu=-.2
surf(X2,Y2,Z2,'EdgeColor','None','FaceColor',[.3 .7 .3],'
    FaceAlpha',.7)

x = -2:.01:2;
% intersection of green and blue surfaces (below)
plot3(x,(1/slope_stab_man)*x.^2,x.^2,'-g','LineWidth',2)
% intersection of red and blue surfaces (below)
plot3(x,x.^2,x.^2,'--r','LineWidth',2)
```

```
plot3(x,x.^2,-1+0*x,'r--','LineWidth',2);

%% Plot Koopman Trajectories (from lines 15-17)
plot3(yA(:,1),yA(:,2),-1+0*yA,'k-','LineWidth',1);
plot3(yB(:,1),yB(:,2),-1+0*yB,'k-','LineWidth',1);
plot3(yC(:,1),yC(:,2),-1+0*yC,'k-','LineWidth',1);
plot3(yA(:,1),yA(:,2),yA(:,3),'k','LineWidth',1.5)
plot3(yB(:,1),yB(:,2),yB(:,3),'k','LineWidth',1.5)
plot3(yC(:,1),yC(:,2),yC(:,3),'k','LineWidth',1.5)
plot3([0 0],[0 0],[0 -1],'ko','LineWidth',4)
set(gca,'ztick',[0 1 2 3 4 5])
axis([-4 4 -1 4 -1 4])
xlabel('y_1'), ylabel('y_2'), zlabel('y_3');
```